OUKA
The University of Osaka
Institutional Knowledge Archive

Title	Metallurgical mechanism of ductility-dip cracking in multipass welds of alloy 690
Author(s)	Okauchi, Hironori; Nomoto, Yuki; Ogiwara, Hiroyuki et al.
Citation	Transactions of JWRI. 2010, 39(2), p. 221-223
Version Type	VoR
URL	https://doi.org/10.18910/4632
rights	
Note	

The University of Osaka Institutional Knowledge Archive : OUKA

https://ir.library.osaka-u.ac.jp/

The University of Osaka

Metallurgical mechanism of ductility-dip cracking in multipass welds of alloy 690†

OKAUCHI Hironori *, NOMOTO Yuki *, OGIWARA Hiroyuki *, SAIDA Kazuyoshi * and NISHIMOTO Kazutoshi *

KEY WORDS: (Alloy 690) (Multipass weld metal) (Microcracking susceptibility) (Impurity elements) (Grain boundary segregation) (Molecular orbital calculation) (Cracking mechanism)

1. Introduction

A Ni-base superalloy, alloy 690 is highly susceptible to ductility-dip cracking, and the primary cause of ductility-dip cracking in the reheated weld metal of alloy 690 is likely to be the reduction of hot ductility attributable to grain boundary segregation of impurity elements such as P and S [1]. The objective of the present study is to clarify the cause of the increased ductility-dip cracking susceptibility with an increase in the P and S contents based on a grain boundary segregation analysis and a molecular orbital analysis of the binding strength of the grain boundary.

2. Materials and Experimental Procedures

The base metal used is a commercial alloy 690. Several kinds of commercial filler metals (FM1-FM3), lab-melting filler metals (FF1-FF5) and extra high-purity filler metal (EHP) were employed for comparison. The chemical compositions of base metal and filler metals used are shown in **Table 1**. The ductility-dip cracking susceptibility in the reheated weld metal was evaluated by the spot-Varestraint test.

Table 1 Chemical compositions of steels used (mass%)

Material		C	Si	Mn	Ni	Cr	Co	Mo	Ti	Al	Fe	P*	S*	B*	Others
Base metal	Alloy 690	0.020	0.12	0.26	Bal.	29.55	0.03	0.02	0.11	0.09	9.61	90	20	<10	-
Filler metal	FE1	0.020	0.15	0.27	Bal.	29.59	0.05	0.02	0.406	0.216	10.13	21	9	<1	-
	FE2	0.022	0.17	0.27	Bal.	29.78	0.05	0.02	0.423	0.214	10.15	19	18	2	-
	FE3	0.022	0.19	0.26	Bal.	29.76	0.05	0.02	0.421	0.224	10.12	20	31	<1	-
	FE4	0.019	0.18	0.27	Bal.	29.87	0.05	0.02	0.420	0.248	10.14	34	11	<1	-
	FE5	0.018	0.22	0.26	Bal.	29.93	0.05	0.02	0.410	0.235	10.14	43	13	<1	-
	FF1	0.020	0.28	0.25	Bal.	29.15	0.024	0.039	0.17	0.092	11.05	50	16	<1	-
	FF2	0.020	0.0036	0.24	Bal.	29.63	0.0004	0.0046	0.22	0.130	10.74	20	36	<1	-
	FF3	0.008	0.078	0.076	Bal.	29.55	0.0004	0.0014	0.36	0.210	10.59	9	37	12	-
	FF4	0.010	0.053	0.081	Bal.	29.89	0.0006	0.0039	0.35	0.160	10.12	30	2	19	-
	FF5	0.015	0.086	0.076	Bal.	29.68	0.0150	0.0230	0.39	0.210	10.97	20	1	24	-
	EHP	0.0019	0.01	<0.01	Bal.	28.92	0.02	0.01	0.09	0.09	10.0	9	8	-	-
	FM1	0.02	0.09	0.80	Bal.	30.06	0.027	0.01	0.224	0.11	8.22	20	10	-	-
	FM2	0.02	0.03	0.81	Bal.	30.04	0.007	0.02	0.210	0.10	10.31	20	10	-	Nb+Ta:0.83
	FM3	0.01	0.11	0.10	Bal.	29.06	-	0.01	0.390	0.21	9.9	20	5	-	Nb:0.05

* : ppm

3. Effects of P and S on Ductility-Dip Cracking

The relationship between (P+1.2S) content in the weld metals and the DTR evaluated is shown in **Fig. 1**. Open and filled symbols indicate crack-free and cracking in the multipass weld cracking test, respectively. There is a good linear relationship between the compositional parameter of (P+1.2S) and the DTR for all weld metals. According to the multipass weld cracking test results, the critical DTR where microcracks didn't occur during multipass welding could be estimated as approx. 200K. It follows that the amount of (P+1.2S) in the weld metal should be limited to 30ppm in order to prevent ductility-dip cracking in the multipass weld metal.

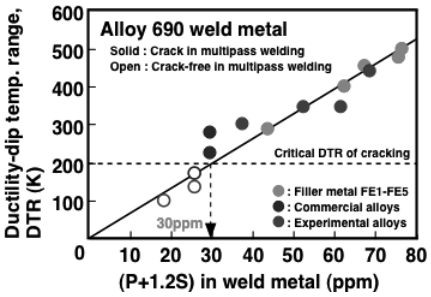

Fig. 1 Relation between (P+1.2S) in weld metal and ductility-dip temperature range, DTR

4. Grain Boundary Segregation of P and S

Numerical Model of Grain Boundary Segregation

The numerical model of microsegregation involves segregation during the solidification stage and segregation/ desegregation during the cooling/reheating stage following solidification in welding under the initial

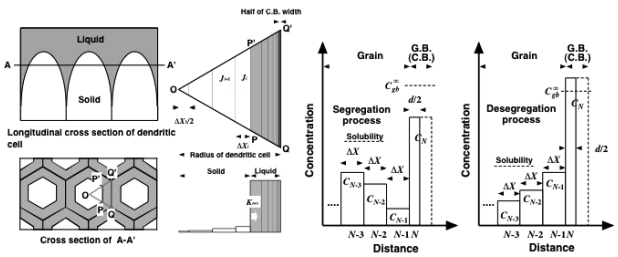

Fig. 2 Schematic illustration of analysis model of microsegregation during multipass welding

† Received on 30 September 2010

* Dept. of Materials & Manufacturing Science, Graduate School of Eng., Osaka University, Osaka, Japan

Transactions of JWRI is published by Joining and Welding Research Institute, Osaka University, Ibaraki, Osaka 567-0047, Japan

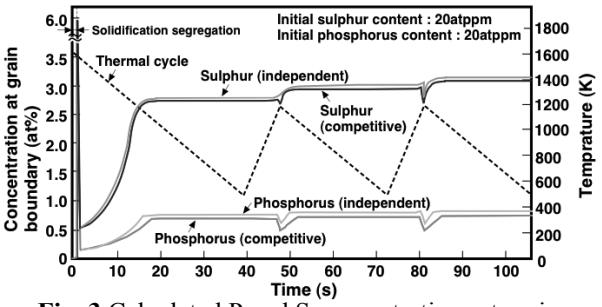

Fig. 3 Calculated P and S concentrations at grain boundary during multipass welding

condition of an inhomogeneous distribution formed by solidification segregation. The solidification segregation behaviours of P and S were calculated for pseudo-binary systems of (Ni-30%Cr-10%Fe)-P and -S. The cosegregation effect of P with S was considered in the equilibrium grain boundary segregation using pseudo-ternary systems of (Ni-30%Cr-10%Fe)-P-S. The distribution of solutes during solidification was determined by the non-equilibrium solidification segregation theory, and that in the solid phase during cooling/reheating processes was calculated by the equilibrium cosegregation theory. The one-dimensional diffusion model in a regular triangle assuming that the morphology of dendrite is basically a hexagonal prism, as shown in **Fig. 2**.

Grain Boundary Segregation Behaviour of P and S

A computer simulation was carried out with the peak temperatures in the 2nd and 3rd cycles being 1200 K. **Figure 3** shows the relation between the elapsed time in multiple welding thermal cycles and the calculated P and S concentrations at the grain boundary. In this figure, the calculated P and S concentrations without considering the cosegregation effect (*i.e.*, "independent segregation") are also depicted. The P and S concentrations at the grain boundary allowing for cosegregation were slightly reduced compared with those in independent segregation because of the competitive effect between P and S. However, similar changes can be seen in the grain boundary concentrations for both situations. Namely, in the solidification process, the P and S concentrations in the liquid phase increased with the progress of solidification, and were rapidly reduced to their equilibrium concentrations (desegregation) when the weld metal was cooled down. However, they increased again at lower temperatures and were saturated at constant values below about 1000 K. In the reheating process, the P and S concentrations at the grain boundary slightly increased during the cooling stage in the reheating process, and afterwards changed cyclically with each thermal cycle. The grain boundary concentration of S during multipass welding was relatively higher than that of P even when their initial contents were identical. Furthermore, the P and S concentrations at the grain boundary slightly increased with an increase in the number of thermal cycles employed. This fact suggests that grain boundary segregation of S as well as P would be promoted by the multiple thermal cycles occurring during multipass welding.

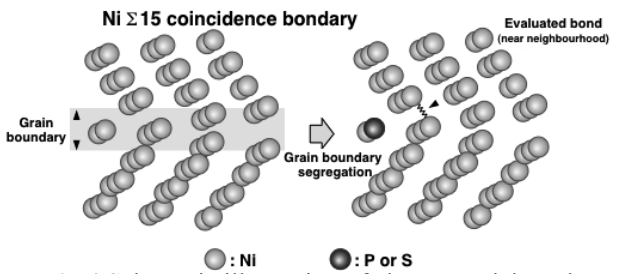

Fig.4 Schematic illustration of cluster model used (molecular orbital analysis by DV-Xα method)

5. Grain Boundary Embrittlement due to P and S Analysed by Molecular Orbital Method

The binding strength of the grain boundary was numerically analysed by a molecular orbital analysis (DV-Xα method). **Figure 4** schematically illustrates the cluster model used in the present computation, the Σ15 coincidence boundary of Ni consisting of 67 atoms. One or two Ni atoms on the grain boundary were replaced by P or S atoms to simulate grain boundary segregation. The binding strength of the grain boundary was evaluated from the bond order between intergranular and intragranular Ni atoms in the near neighbourhood of P and S atoms. The calculated bond orders of Ni atom at the grain boundary for different segregation situations are shown in **Fig. 5**. Ni_{67} indicates the non-segregated situation, $Ni_{66}X_1$ and $Ni_{65}X_2$, $Ni_{65}X_1Y_1$ (X, Y=P, S) indicate the segregated situations where one and two intergranular Ni atoms were replaced by an X and/or Y atom, respectively. When P and S were segregated at the grain boundaries, the bond orders of the Ni atoms were reduced compared to the non-segregated situation, and it decreased with an increase in the number of segregated P and S atoms. The bond orders of the Ni atoms when S was segregated to the grain boundary were lower than those for P segregation. However, the fact that the calculated bond order of Ni atom in $Ni_{65}P_1S_1$ ranked between $Ni_{65}P_2$ and $Ni_{65}S_2$ prevented the confirmation of any discernible effect of cosegregation of P with S in the present analysis.

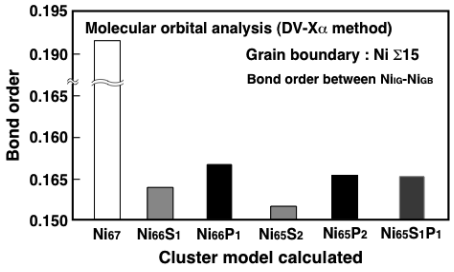

Fig.5 Calculated bond order between Ni atoms for different grain boundary segregation scenarios

6. Mechanism of Ductility-Dip Cracking in Multipass Weld

A grain boundary segregation analysis revealed that P and S (especially S) were segregated to the grain boundary in the weld metal during multipass welding. A molecular orbital analysis suggests a possibility that grain boundary segregation of P and S leads to grain boundary embrittlement. It follows that the ductility-dip cracking in the reheated weld metal of alloy 690 would be dominantly caused by the embrittlement of grain boundaries resulting from the imbalance between intergranular strength and intragranular strength at high temperature attributable to grain boundary segregation of impurity elements such as P and S.

7. Conclusions

(1) A numerical analysis of the segregation behaviours of P and S revealed that these elements were cosegregated at the grain boundary during multipass welding. P and S concentrations at the grain boundary slightly increased with an increase in the number of thermal cycles applied.
(2) A molecular orbital analysis suggested a possibility that grain boundary segregation of P and S led to grain boundary embrittlement.

References

[1] K.Nishimoto, K.Saida, H.Okauchi and K.Ohta : Sci. and Technol. of Welding and Joining, 11-4 (2006), p.462-470.